

# A high-resolution model of the Hydrodynamics of the whole Great Barrier Reef

Jonathan Lambrechts<sup>a</sup>, Emmanuel Hanert<sup>b</sup>, Eric Deleersnijder<sup>c,a</sup>,  
Paul-Emile Bernard<sup>a</sup>, Vincent Legat<sup>a</sup>, Jean-François Remacle<sup>d,a</sup>  
and Eric Wolanski<sup>e</sup>

<sup>a</sup> *Université catholique de Louvain, Centre for Systems Engineering and Applied  
Mechanics B-1348 Louvain-la-Neuve, Belgium*

<sup>b</sup> *The University of Reading, Department of Meteorology, Earley Gate, PO Box 243,  
Reading RG6 6BB, UK*

<sup>c</sup> *Université catholique de Louvain, Institut d'Astronomie et de Géophysique G. Lemaître,  
B-1348 Louvain-la-Neuve, Belgium*

<sup>d</sup> *Université catholique de Louvain, Département de Génie Civil et Environmental, B-1348  
Louvain-la-Neuve, Belgium*

<sup>e</sup> *Australian Institute of Marine Science (AIMS), PMB No. 3, Townsville MC, Queensland,  
4810 Australia*

---

## Abstract

An unstructured-mesh parallel hydrodynamical model of the whole Great Barrier Reef is presented. The depth-averaged equations of motion are discretized in space by means of a mixed finite element formulation while the time marching procedure is based on a third order explicit Adams-Bashforth scheme. The mesh is made up of triangles. The size and the shape of the triangles can be modified easily so as to resolve a wide range of scales of motion, from those of the regional flows to those of the eddies or tidal jets that develop in the vicinity of reefs and islands. The forcings are the surface wind stress, the tides and the East Australian Current, the latter two forcings being applied along the open boundaries of the computational domain. The numerical results compare favourably with observations of both alongshores currents due to the East Australian Current and the local perturbations due to narrow reef passages. Comparisons are also performed with the simulations of a three-dimensional model applied to a small domain centered on Rattray Island, showing that both models produce similar flow fields. For a structured-mesh model to yield results of the same accuracy, it is likely that the computational cost would be much higher.

*Key words:* Great Barrier Reef, Hydrodynamics, Shelf Dynamics, Finite Elements, Unstructured Mesh, East Australian Current.

---

## 1 Introduction

The Great Barrier Reef is on the continental shelf of Australian northeastern coastline as illustrated in Figure 1. Typically, there are over 2500 coral reefs along 2600 *km*. Due to recent human activities, these ecosystems deteriorate at an alarming rate. Land use contributes to degradation of the health of the Great Barrier Reef and to an increased frequency and intensity of crown-of-thorns starfish infestations (Wolanski and De'ath, 2005; Richmond et al., 2007). Recent analysis suggest that if global warming proceeds unchecked, biological adaptation is the only possible savior of the ecosystem. Therefore, there is a strong need for accurate hydrodynamical simulations allowing to better understand and analyse the interactions between ecological processes and human impacts (Veron, 1995; Birkeland, 1997; Wilkinson, 1999; Richmond, 1993; Wolanski, 2001). Today, developing an high-resolution, efficient and realistic model of the hydrodynamics of the whole Great Barrier Reef is still a difficult task in view of the complex bathymetry and topography. Taking up this challenge is the objective of the present study.

The circulation over the Great Barrier Reef shelf is mainly controlled by the complex topography, the local wind, the tidal motions and the shoreward South Equatorial Current in the western Coral Sea. On meeting the continental slope of the Great Barrier Reef, this current splits at a bifurcation point between  $14^{\circ}S$  and  $18^{\circ}S$  into the northward-flowing Coral Sea Coastal Current and the southward-flowing East Australian Current (Wolanski, 1994). These longshores currents are modulated and deviated by the wind, the tides and the topography, which can strongly deflect the mean current away from areas of high reef density. The mean current is an essential ingredient of the ecosystem as it flushes the shelf and controls the dominant spreading direction of material emanating from reefs (Wolanski and Spagnol, 2000; Brinkman et al., 2001; Wolanski et al., 2003b; Luick et al., 2007). In other words, it controls the connectivity of reef populations as a result of the transport of water-borne larvae between reefs (Wolanski et al., 1997; Armsworth and Bode, 1999; Wolanski et al., 2004) or the transport of nutrients and pollutants by water currents (Done, 1988; Bell and Elmetri, 1995; Wolanski et al., 1999). Moreover, tidal jets and eddies occur in the wake of islands and have also a significant impact on the ecosystem. Their length scales range from about hundred meters to a few kilometers. In situ measurements, satellite imagery and numerical simulations show that those small-scale phenomena are mainly confined to the neighbourhood of small reefs, islands and passages (Hamner and Hauri, 1981; Wolanski and Hamner, 1988; Wolanski et al., 1988; Deleersnijder and Beckers, 1992; Wolanski et al., 1996).

These abovementioned processes occur over a wide range of space and time scales, from a few meters to hundreds of kilometers, and from a few seconds to several years (Wolanski et al., 2003c). It is essential to simultaneously simulate all scales of the motion, because small- and large-scale processes exhibit significant inter-

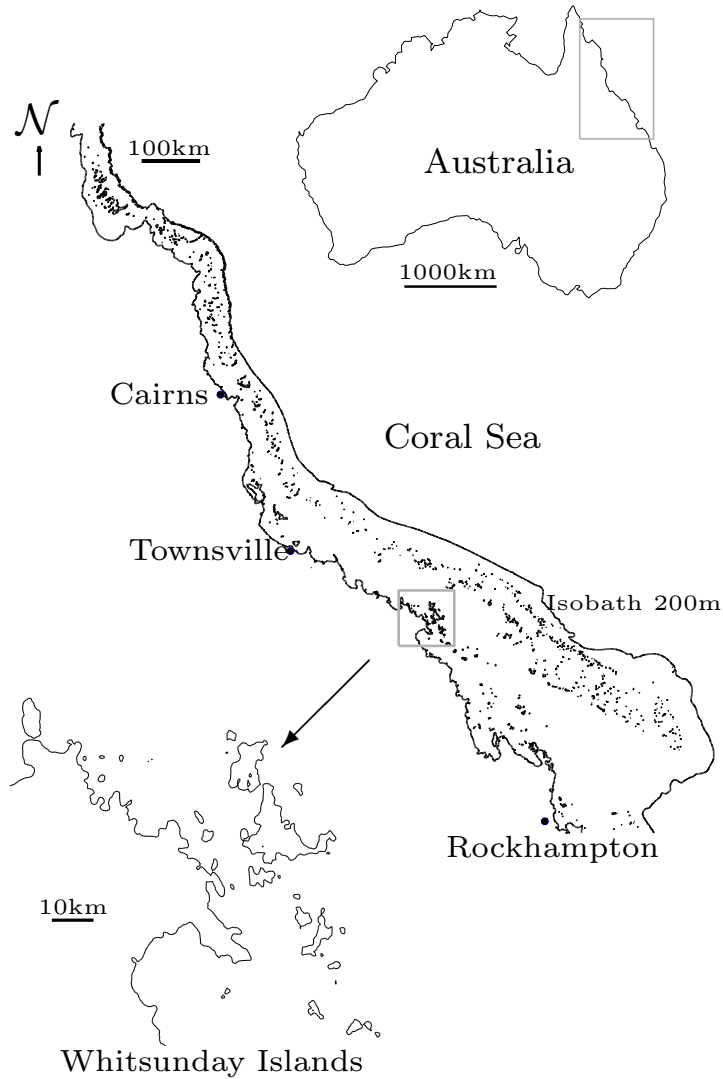


Figure 1. Locality map of the whole Great Barrier Reef. The model computational domain is located between the coastline and the continental shelf break defined by the isobath of 200 *m*. A close-up view of Whitsunday Islands illustrates the complexity of the topography.

action (Wolanski et al., 2003c). Clearly, a model focusing on a single phenomena while ignoring others, may lead to misleading results. However, all scales of the motion cannot be reproduced by the state-of-the-art structured uniform grid models of the Great Barrier. Typically, the cell size of these models is around 2000 *m* (King and Wolanski, 1996; Brinkman et al., 2001), i.e. quite larger than the characteristic sizes of a whole class of biological and hydrodynamic processes. For a uniform grid model to reproduce small-scale processes such as eddies and tidal jets, the computational cost is likely to be crippling. This is why variable resolution is needed. This could be achieved by having recourse to nested grids (Spall and Holland, 1991; Fox and Maskell, 1995). However, the regions where enhanced resolution would be needed are so numerous in the Great Barrier that this approach

is unlikely to be feasible. Therefore, the parallel model developed herein is based on an unstructured, variable-resolution mesh that offers an very strong geometrical flexibility (Walters, 2005; Pietrzak et al., 2005; Legrand et al., 2006).

This paper is organized as follows. In section 2, the model is outlined, while Section 3 focuses on important numerical aspects. The results are discussed in Section 4.

## 2 Unstructured Hydrodynamical Model

Using the same mathematical frameworks as the previous structured grids models (Wolanski et al., 1996; Brinkman et al., 2001) , a depth-averaged barotropic model is implemented to derive the mean horizontal vector  $\mathbf{u} = (u, v)$  and the sea surface elevation  $\eta$ . Unlike previous models, the equations are here discretized on a fully unstructured grid of approximately 850.000 elements depicted in Figure 2. The mesh resolution ranges from 150 meters along tiny islands to ten kilometers in open areas: it allows us to take advantage of each degree of freedom as a high resolution model is introduced only where the flow features require it. The local resolution is often quite finer than the grid cell of two kilometers used in the simulations of (Brinkman et al., 2001) .

Paradoxally, the ability of the grid to represent the reef scales could make irrelevant the assumption that a depth-averaged barotropic model is still appropriate for this application. When the grid size is larger than one kilometer, the shallow waters equations can be used to simulate the flow as in those length scales, the shelf water are generally well mixed throughout the year and that the flow is primarily horizontal as pointed by (Brinkman et al., 2001; Wolanski, 1994). At the reef scale, three-dimensional features, like the eddies in the wake of islands, can no longer be neglected. Both experimental observations and numerical simulations reveal that these eddies have a full three-dimensional structure that creates some strong upwelling in their centre and even stronger downwelling along their edges (Wolanski, 1994; White and Deleersnijder, 2006). Moreover, if the element size is of the order of the local water depth, non-hydrostatic effects can no longer be neglected and an hierarchical modelling should be introduced to accurately represent the hydrodynamics of the Great Barrier Reef over a broad range of scales. Such an approach is a very ambitious task that would require numerous validations, comparisons and tailored parameterizations (Wolanski et al., 1996). It must also pointed out that several authors claim that two-dimensional models produce very accurate and physically relevant results even for the tidal circulation in island's wakes or headland eddies (Pattiaratchi et al., 1986; Falconer et al., 1986), because the depth is small and the water column is well mixed. Therefore, this paper has to be considered as a first step in the direction where we only introduce a highly graded resolution with the same depth-averaged model. In other words, very localised, reef-induced three-dimensional circulation features that occur at the smallest scales of the grid

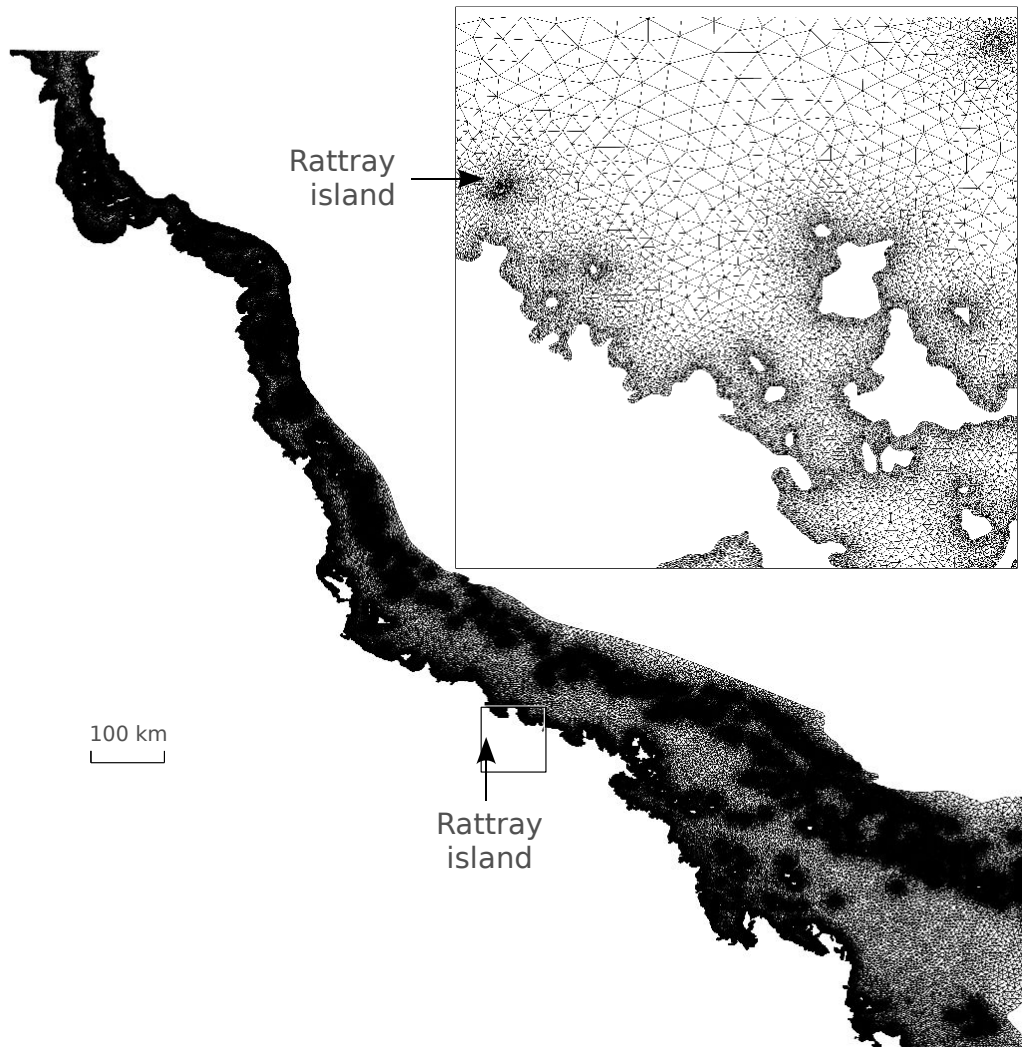


Figure 2. Mesh of the Great Barrier Reef with a close up views illustrating the large range of element sizes. The minimal and the maximal mesh sizes are 150 *m* and 10 *km*, respectively. The number of elements and nodes are 850 843 and 500 142.

(Wolanski and Hamner, 1988; Deleersnijder and Beckers, 1992; Wolanski et al., 1996) are perhaps well simulated by a two-dimensional model, but this ability has to be confirmed by comparison with experiments or three-dimensional calculations. The second step would then consist in defining and coupling a family of mathematical models ranging from the depth-averaged two-dimensional equations to the full set of the three-dimensional Navier-Stokes equations.

The model domain has been defined in the whole area where we have accurate bathymetrical data. Basically, it covers almost the whole Great Barrier Reef from the Great Keppel Island in the south, to the Forbes Island in the north. The area of the computational domain is almost two times larger compared to the previous simulations (Brinkman et al., 2001).

In a two-dimensional, depth-averaged shallow water model, the mass and momentum conservation equations read:

$$\left\{ \begin{array}{l} \frac{\partial \eta}{\partial t} + \frac{\partial H u}{\partial x} + \frac{\partial H v}{\partial y} = 0, \\ \frac{\partial u}{\partial t} + u \frac{\partial u}{\partial x} + v \frac{\partial u}{\partial y} - f v + g \frac{\partial \eta}{\partial x} = \frac{\nu}{H} \left( \frac{\partial}{\partial x} \left( H \frac{\partial u}{\partial x} \right) + \frac{\partial}{\partial y} \left( H \frac{\partial u}{\partial y} \right) \right) + \frac{\tau_x}{\rho H} - \frac{\gamma \|\mathbf{u}\|}{H} u, \\ \frac{\partial v}{\partial t} + u \frac{\partial v}{\partial x} + v \frac{\partial v}{\partial y} + f u + g \frac{\partial \eta}{\partial y} = \frac{\nu}{H} \left( \frac{\partial}{\partial x} \left( H \frac{\partial v}{\partial x} \right) + \frac{\partial}{\partial y} \left( H \frac{\partial v}{\partial y} \right) \right) + \frac{\tau_y}{\rho H} - \frac{\gamma \|\mathbf{u}\|}{H} v, \end{array} \right. \quad (1)$$

where  $H = h + \eta$  is the total water depth, and  $h$  is the water depth below the mean sea level. The Coriolis parameter, the acceleration due to gravity, the horizontal eddy viscosity, the mean water density are respectively denoted by  $f$ ,  $g$ ,  $\nu$  and  $\rho$ . At the surface of the sea, the wind stress is given by  $\boldsymbol{\tau} = (\tau_x, \tau_u)$ . At the bottom, the friction is parametrized with a quadratic closure relationship where  $\gamma$  is a dimensionless friction coefficient and  $\|\mathbf{u}\|$  represents the amplitude of the velocity. Those partial differential equations have to be supplemented with mathematically relevant initial and boundary conditions in order to define a well-posed boundary value problem and to produce reliable predictions. The influence of the initial conditions becomes negligible after some time, due to frictional and viscous dissipations. Co-oscillating tides may be generated from any initial state if a sufficient time is given allowing the tidal solution to become established.

On one hand, a vanishing mass flux and a tangential depth-averaged momentum proportional to the mean tangential velocity is imposed along the coastline and the islands :

$$\left\{ \begin{array}{l} u_n = 0, \\ \nu \frac{\partial u_s}{\partial n} - \alpha u_s = 0, \end{array} \right. \quad (2)$$

where the indices  $s$  and  $n$  denote the tangential and the normal outward directions along the boundary. The symbols  $u_s$  and  $u_n$  are the components of the depth averaged horizontal velocity along those directions. This boundary condition amounts to parameterize the unresolved boundary layer along the coasts by an empirical and purely phenomenological partial slip condition. The selection of the parameter  $\alpha$  is based on the knowledge of the flow and remains a relatively tedious technical issue.

On the other hand, imposing conditions on the open part of the boundary is more delicate. As mentioned by Blayo and Debreu (2005), a large number of alternative conditions can be used to introduce the tide and the East Australian Current on an open boundary. A quite naive (but usual) approach would be to specify the elevation as a function of position and time. However, it was observed by Flather (1976), that such an approach is unsatisfactory near the shelf edge, despite numerous experiments with several different ways of implementing the condition. In fact, the best possibility is to prescribe a relationship between elevation and velocity in terms of incoming characteristic variables (Blayo and Debreu, 2005; Reid and Bodine,

1968) and to supplement it by imposing a vanishing depth-averaged shear stress :

$$\begin{cases} \sqrt{\frac{g}{h}}\eta + u_n = \zeta, \\ \nu \frac{\partial u_s}{\partial n} = 0. \end{cases} \quad (3)$$

where the function  $\zeta$  is derived from external data. For the Great Barrier Reef, measurements of the sea elevation at some locations in the Coral Sea can be used to force the tides and the East Australian Current. By assuming a vanishing normal velocity gradient over the boundary, an external normal velocity can be extrapolated from the internal computed flow. Both vanishing stress conditions may look quite arbitrary, but appeared to be the most flexible choice in order to prevent any numerical instabilities. In our model, the whole set of those boundary conditions involves a critical step in the procedure and may dramatically change the numerical predictions. The best way to impose open-sea boundary conditions is still an open area of research.

An approximate solution of the partial differential equations with the boundary conditions is then obtained by using the Finite Element Method that can handle unstructured grids, contrary to the Finite Difference Method. The linear piecewise discretizations is used for both elevation and velocity fields. In order to avoid any spurious numerical modes, we use a discontinuous velocity together with an usual continuous piecewise linear elevation. Typically, such an approximation is known as  $P_1^{nc} - P_1$  element. Details about the mathematical analysis and numerical validation of this element for the shallow water equations is given in (Hua and Thomasset, 1984; Le Roux, 2005; Hanert et al., 2005, 2004). Let us just mention that a peculiar care is required to enforce the boundary conditions in the numerical scheme. Typically, we weakly impose boundary conditions in terms of the characteristic variables of the first-order hyperbolic terms of the equations. We also neglect the non-linear component of the viscous terms in order to improve the efficiency of the calculations. This approach is largely justified by the fact that such an approximation appears to have almost absolutely no impact on the flow features, because  $\eta \ll h$

As time-marching procedure, a third order explicit Adams-Bashforth integration scheme is selected. It is only conditionally stable and appears to be a quite good compromise between simplicity, efficiency and accuracy. In order to take advantage of parallel computing, the mesh is partitioned into sub-domains attributed to each of the processors of a parallel cluster. In Figure 3, the mesh partitioning is obtained to uniformly distribute the computing charge and minimise the communications. The parallel speed-up is defined as the ratio between the elapsed time with one processors and with several processors simultaneously performing the task. An ideal implementation would produce a straight line with an unitary slope, if all time spent in communications could be considered as negligible. The observed speed-up exactly superposes the theoretical ideal curve taking advantage of the fact that

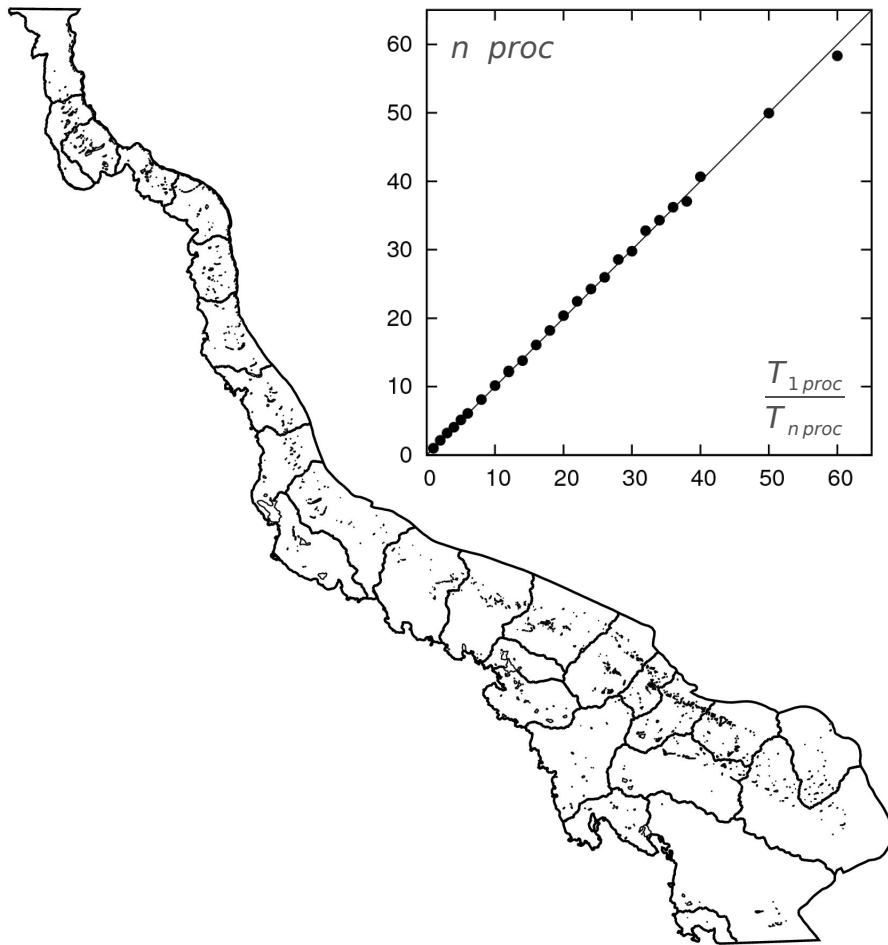


Figure 3. Partition of the mesh into 25 subdomains for parallel computing. The observed speed-up exactly superposes the theoretical ideal curve.

explicit time integration schemes can often be parallelized in a very efficient way.

### 3 Numerical techniques

The first ingredient of the numerical calculations is the design of the unstructured grid. Firstly, it is critical to accurately represent the coastline, the open boundaries and all relevant islands. Secondly, we define the mesh resolution from the physical processes that should be simulated. The mesh are obtained with the `gmsh` software (Remacle, 2007). The resolution of the mesh in Figure 2 depends on two *a priori* criteria:

- The local mesh size has to be proportional to the square root of the bathymetry

in order to obtain the same Courant-Friedrichs-Lewy condition (CFL condition) for the gravity waves over the whole domain. In other words, the element size is adjusted in such a way that the external inertia-gravity waves travel over the same fraction of each element for a given time interval.

- The local mesh size depends on the distance to islands and reefs in order to cluster mesh nodes in regions where small scale processes are taking place. The mesh is refined even more in the proximity of islands where eddies and tidal jets can be expected.

Both criteria are blended together so to have a high resolution in the vicinity of reefs and island and a resolution depending only on the bathymetry elsewhere (Legrand et al., 2006). A more ambitious strategy would be to introduce adaptive meshes. The element size could be dynamically adjusted using an *a posteriori* error estimator from the numerical discontinuities in the solution at the element interfaces (Bernard et al., 2007). A quasi-optimal mesh could then be derived for a whole simulation. Even if it may appear attractive, we think that dynamically adapting the mesh during the time integration would not provide a dramatic improvement as most refinements can be easily predicted a priori. However, such an approach can be useful to deal with moving boundaries due to the wetting and drying of coral reefs.

The second issue is to define the material parameters to represent subgrid effects. Obviously, they must be defined as a function of the local mesh size  $\Delta$ . To incorporate unresolved turbulent features and boundary layers along the coastlines and islands, the value of the horizontal eddy viscosity  $\nu$  and the friction coefficient  $\alpha$  depend on the local mesh size following (Okubo, 1971) :

$$\begin{aligned}\nu &= 1.35 \Delta^{1.15} \quad 10^{-3} \text{ m}^2/\text{s}, \\ \alpha \nu &= 2.5 \quad 10^{-3} \text{ m}^2/\text{s}^2,\end{aligned}\tag{4}$$

The last item consists in defining the external forcings of the hydrodynamics of the Great Barrier Reef: the wind, the adjacent Coral Sea circulation and the tides. Wind data are extracted from the NCEP reanalysis data provided by the NOAA/OAR/ESRL PSD, Boulder, Colorado, USA. (Kalnay et al., 1996). The stress acting on the sea from the wind is modelled by using the parametrization proposed by Smith and Banke (1975) :

$$\boldsymbol{\tau} = 10^{-3} \underbrace{\left(0.630 \|\mathbf{v}_w\| + 0.066 \|\mathbf{v}_w\|^2\right)}_{C(\mathbf{v}_w)} \mathbf{v}_w,\tag{5}$$

where  $\mathbf{v}_w$  is the surface wind velocity in  $m/s$  and  $C(\mathbf{v}_w)$  is a scaling parameter in  $kg/m^2s$ . To incorporate the effect of the East Australian Current coming from the

Coral Sea and the tides, we have to specify the elevation  $\eta_{sea}(x, y, t)$  on the open-sea part of the boundary. The measurements of the elevations at several locations accurately provides the tidal dynamics, but the global East Australian Current effect is largely covered by noise and long term fluctuations. Therefore, we prescribe the elevation at the open-sea boundary as follows :

$$\eta(x, y, t) = \bar{\eta}(x, y) + \eta'(x, y, t) \quad (6)$$

where  $\eta'(x, y, t)$  is the temporal variations of the measurement of the sea level in the Coral Sea and  $\bar{\eta}(x, y)$  is a steady-state elevation imposed to obtain the East Current in the flow domain in a time-averaged sense. The temporal variations of the tidal elevation on the north-western, eastern and south-eastern open boundaries are obtained by a linear interpolation from 15 measurement sites where the National Australian Time Tables provide the elevation and phase shift of the 12 principal tidal constituents. As the amplitude of the temporal variations is quite larger than the variations of  $\bar{\eta}(x, y)$ , it appears unwise to have confidence to the constant part of the data. Moreover, large scale features also are included in those data and render them incompatible with the assumption of a spatially established flow along the boundary.

In order to circumvent this incompatibility leading to a wrong solution, we use an auxiliary steady-state problem to identify the suitable form of the function  $\bar{\eta}(x, y)$ . This auxiliary problem consists in using the East Australian Current as the unique forcing in terms of velocity along the whole boundary. Opposite flows are induced by prescribing the longshore velocity at the upper and a lower parts of the open-sea boundary. In an intermediate neutral area, we define an zone of incoming cross-shore current separating them. Dividing the boundary in such a way may be considered as arbitrary. However, it can be justified by a good intuition from the observations (Brinkman et al., 2001) . When the steady state flow is reached, the surface elevation on the boundaries is considered as the good candidate to enforce the East Australian Current.

As the problem is not linear and as the tidal motions generate a larger amount of dissipation, it is necessary to multiply the steady-state solution to get the adequate  $\bar{\eta}(x, y)$  by a scalar factor in order to obtain the correct mean flow when the time average is performed. Typically, this factor ranges from 2 to 3. It must be pointed out that this approach is a purely phenomenological way to close the problem and to enforce large scale flow features in the computational domain. This approach is the less stringent way to enforce the East Australian Current and seems to be less invasive than the strategy proposed by Brinkman et al. (2001). The global East Australian Current is taken into account by adding a global surface elevation gradient pointing northward in the northern part of the domain and southward in the southern part. In that case, the mean flow is forced on the whole domain in a very strong way and is often incoherent with the Coriolis effects occurring in the domain.

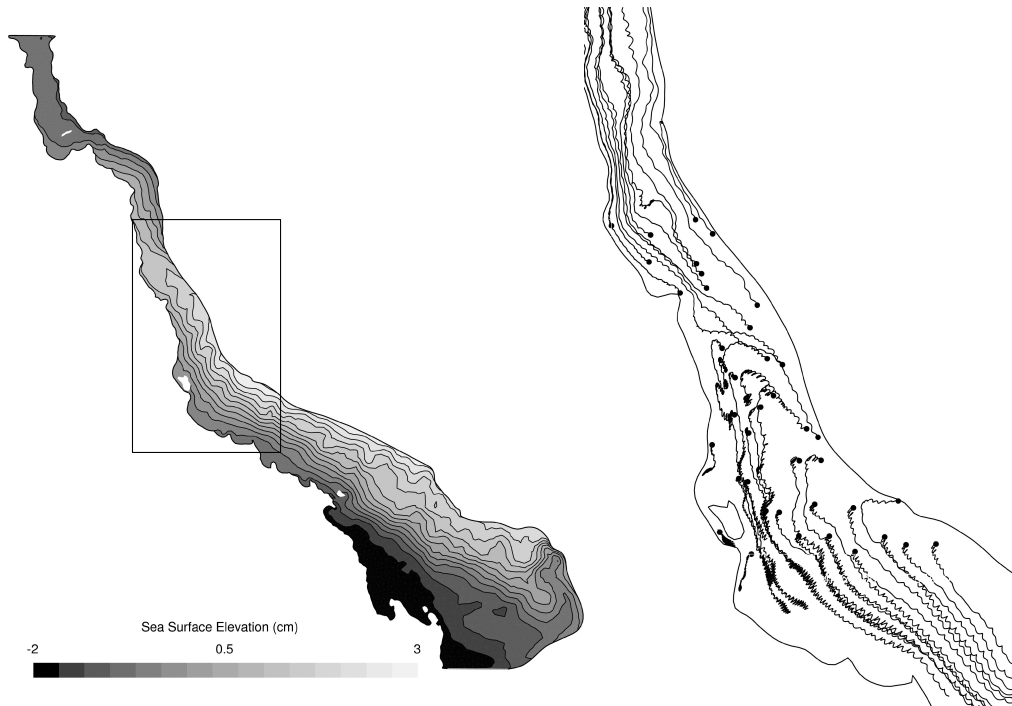


Figure 4. On the left side of the Figure, contourlines of the mean sea surface elevation  $\bar{\eta}(x)$  obtained with the auxiliary steady-state problem and used as prescribed mean elevation at the open boundary are given. The elevation only varies in the long-shore direction in the central part of the Great Barrier Reef while it is in the cross-shore direction elsewhere. On the right side of the Figure, several trajectories of Lagrangians particles are drawn. Both tidal motions and global East Australian Current effects can be easily identified. The separation of the oceanic inflow into two branches also occurs at a location corresponding to current meter data.

As the angle between the gradient direction and the equilibrium velocity depends on the Coriolis factor, the bathymetry and the local topography, such a complex relationship has to be estimated to address this issue. It is a quite challenging task that was not performed. The final technique proposed by Brinkman et al. (2001) consists in more constraining the flow by prescribing a geostrophic balance at the open sea boundaries. We believe that our strategy defines a quite better well-posed problem and also reduces, in a dramatic way, the constraints to the flow. Let us again recall that those constrains resulting from closure considerations are always the most prominent and remaining part of the modeling procedure.

#### 4 Discussion

Low-frequency, longshore currents are well predicted by the model, as shown in Figure 4 where the trajectories of some Lagrangian particles illustrate both the tidal variations and the long term flow. Such an observation can be expected as we are

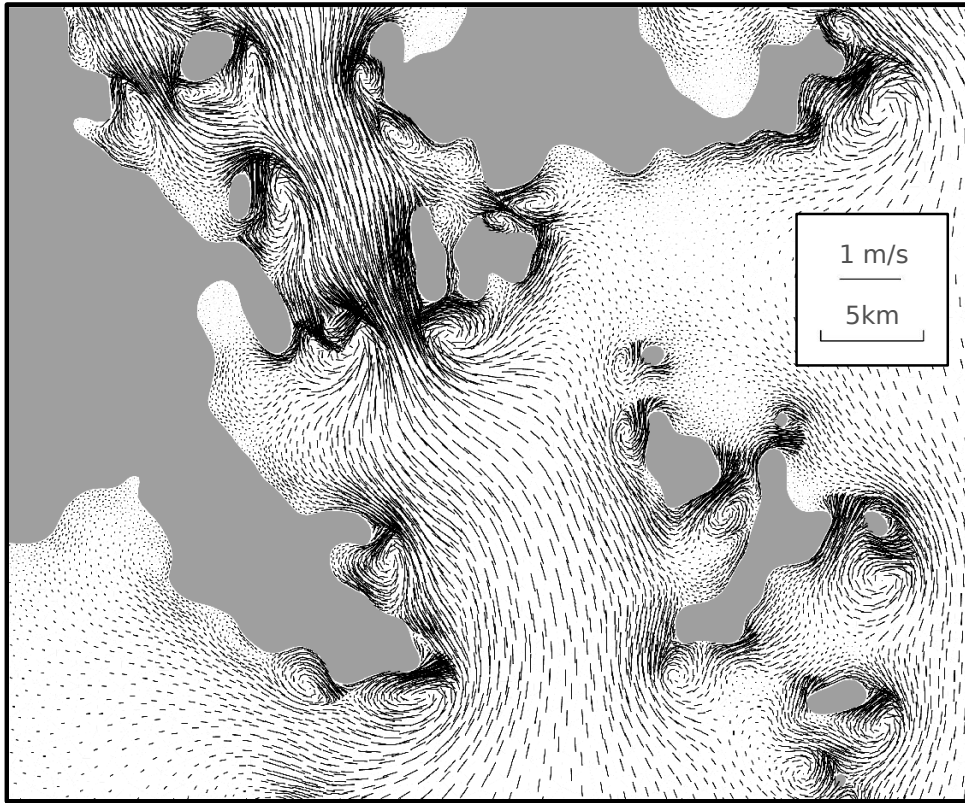


Figure 5. Sticky water in the south of the Withsundays Islands ( $20^{\circ}21'S$   $149^{\circ}00'E$ ). The typical size of the islands is a few kilometers. The mesh resolution is about 200 meters.

specifically forcing the model to get it right. More critical is the model ability to represent a broad range of scales : let us just cite the tide as a propagating wave over the shelf described by (Wolanski and Hamner, 1988), the eddies and tidal jets created by the topography. The model demonstrates the existence of macro-turbulence in the Great Barrier Reef, due to the interaction of the tidal currents with many islands and reefs acting together to generate large-scale sticky water effect (Wolanski and Spagnol, 2000; Spagnol et al., 2001). This also demonstrates a feedback process whereby the small-scale processes influence the large scale flows, as discussed by Wolanski et al. (2003a) for one specific area. The sticky water effect, illustrated in Figure 5, is widespread throughout the Great Barrier Reef both in coastal waters as well as in the Great Barrier Reef matrix. This has important biological implications because it demonstrates that the connectivity between various areas will vary according to the reef or island density.

In order to estimate the accuracy of the model, we compare the calculated sea-surface elevation with observations at Pelican Island, Sudbury Cay, Stanley Reef, Karamea Bank and Gannet Cay inside the flow domain. These 5 sites are located in the upper, central and lower parts of the Great Barrier Reef, respectively. Numerical

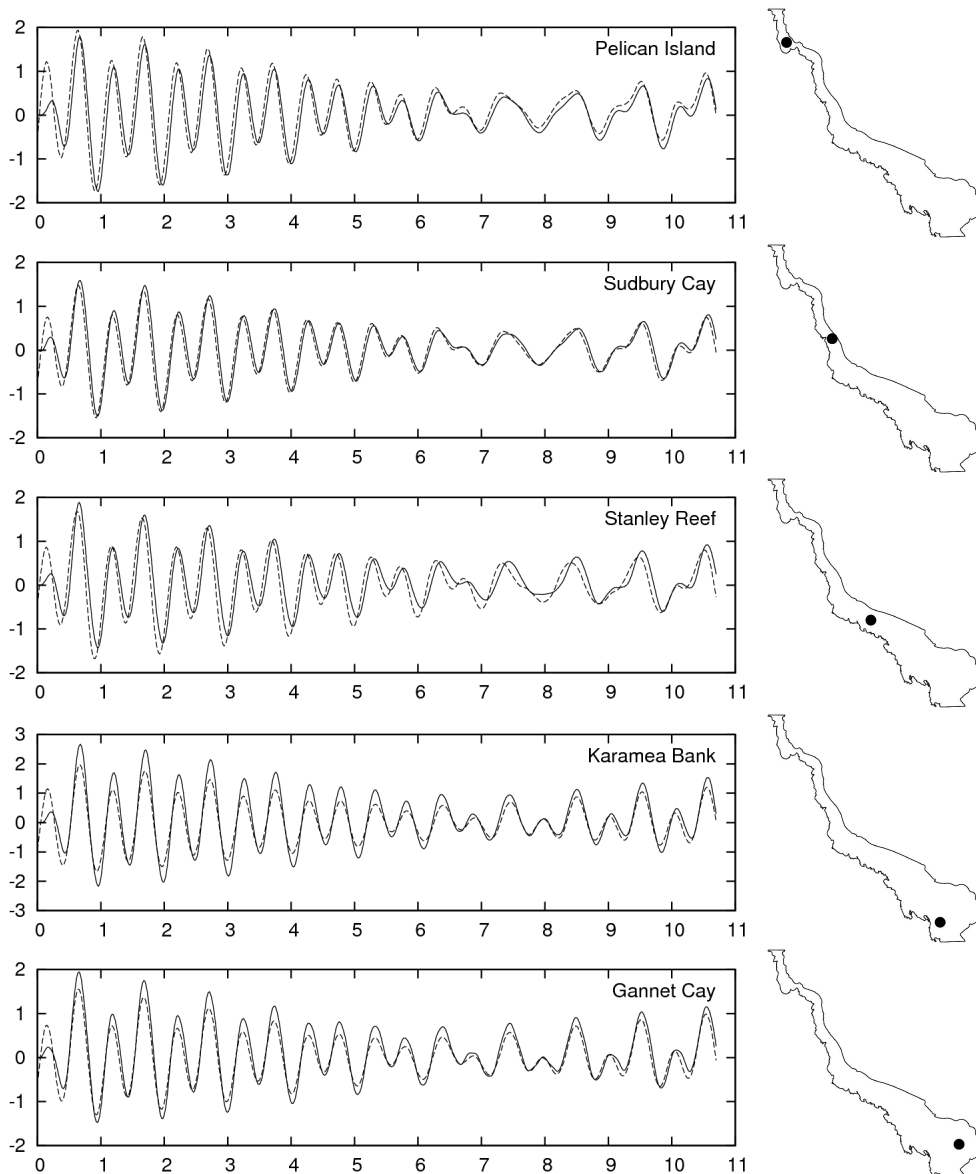


Figure 6. Day series of observed and predicted sea surface elevation (in meters) at measurement sites : Pelican Island, Sudbury Cay, Stanley Reef, Karamea Bank and Gannet Cay. Measured elevation are represented with dashed lines, while the predictions are given in a continuous line.

results and observations are shown in Figure 6. We see a good agreement between the predicted and observed elevations, both in terms of amplitude and phase shift.

It is also quite useful to confront the predicted results with some small scale three-dimensional calculations performed by (White and Deleersnijder, 2006; White and Wolanski, 2007) around Rattray Island. In their calculations, White and Deleersnijder (2006) used a rectangular computational domain of approximately  $100 \text{ km}^2$

and obtained some results that compare favourably with current metering performed by Wolanski et al. (1984). Because of its limited extent, the  $f$ -plane approximation was made. The Smagorinsky parameterization is used to model subgrid effects. The bottom stress was computed by using the mean values of the last two bottom velocity nodes. The surface wind stress can be neglected. At both upper and lower boundaries, the tidal motions were enforced while the lateral boundaries are assumed to be impermeable.

In Figure 7, we compare the eddies that are generated when the flow interacts with Rattray Island, even if the resolutions are quite different. Although, the available bathymetry in our calculations remains too coarse, it mainly appears that the same basic flow features are predicted by both models. Therefore, we could investigate the physics by analysing inertial jets occurring when the flow is accelerated through narrow reef passages. Typically, the unstable resulting jet results in a pair of eddies at the outflow. Those tidal jets can be viewed by this high resolution unstructured model where a mesh refinement along the islands is performed, as illustrated in Figure 8. These mushroom shaped circulation patterns, well predicted when the flow is accelerated between both islands, have been observed on the field by Wolanski (1994). It is also mandatory to keep the numerical diffusion below the physical subgrid diffusion in order to avoid to smooth all the features.

Even if small scales features are well predicted by the model, we must emphasize that the hierarchical adaptive grid does not correspond to a hierarchical mathematical modelling. Basically, we still consider some large scale averaged shallow water equations when the grid refinement implies that the non-hydrostatic processes might not be negligible. A careful analysis of the subgrid closure modelling and parametrization is certainly the next step of our work. However, our simulations show that the complex topography of the Great Barrier Reef introduces major spatial and temporal variability in the net circulation of this region, as mentioned by (Brinkman et al., 2001; King, 1992; King and Wolanski, 1996; Wolanski and Spagnol, 2000). In a quite more illustrative way, this work also demonstrate that the variability of the topographical details strongly influence the magnitude of the small scales features and not only the locations of exchange between the Coral Sea and the Great Barrier Reef. We also demonstrate that a large number of small scale features could be nicely observed and used to better understand the complex flow dynamics of the Reef.

Even if this work has to be considered as a first attempt towards a three-dimensional high-resolution model of the whole Great Barrier Reef, it now appears possible to broaden the range of scales where quite different physical processes occur. Even the flow within a single coral reef is also taking place over a widely broad range of scales (Monismith, 2007). The physics involved undergoes huge changes when going from the size of a coral colony (mm to cm) to the whole reef scale (100 m to 1 km). Of particular interest is the boundary layer flow over the reefs, which is mainly influenced by the complex and porous geometry of the reefs. The resulting

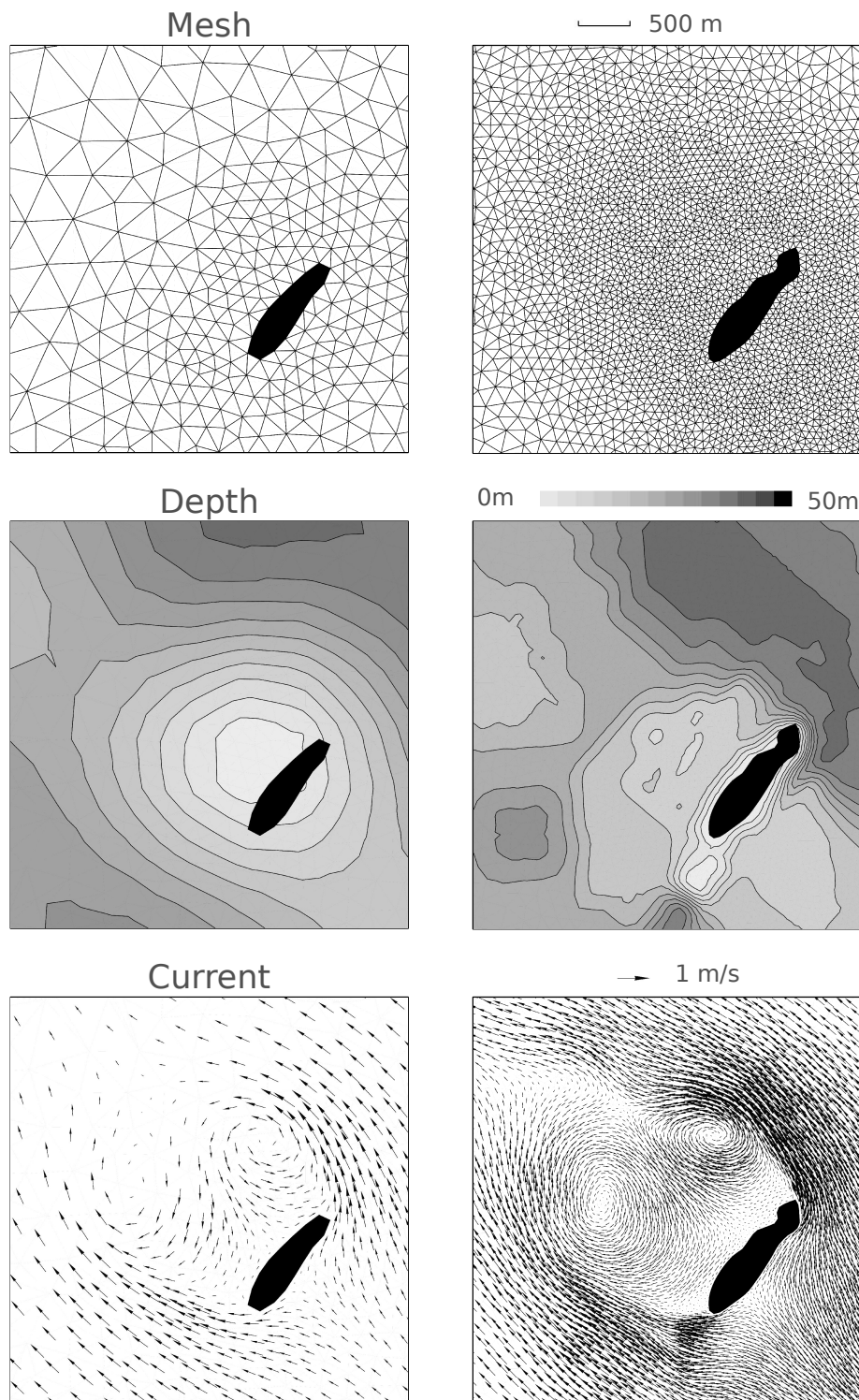


Figure 7. Close-up views of meshes, bathymetrical contourlines and eddies at a given time from our global model and the three-dimensional small scale calculations of White and Deleersnijder (2006) are presented on the left and the right sides, respectively.

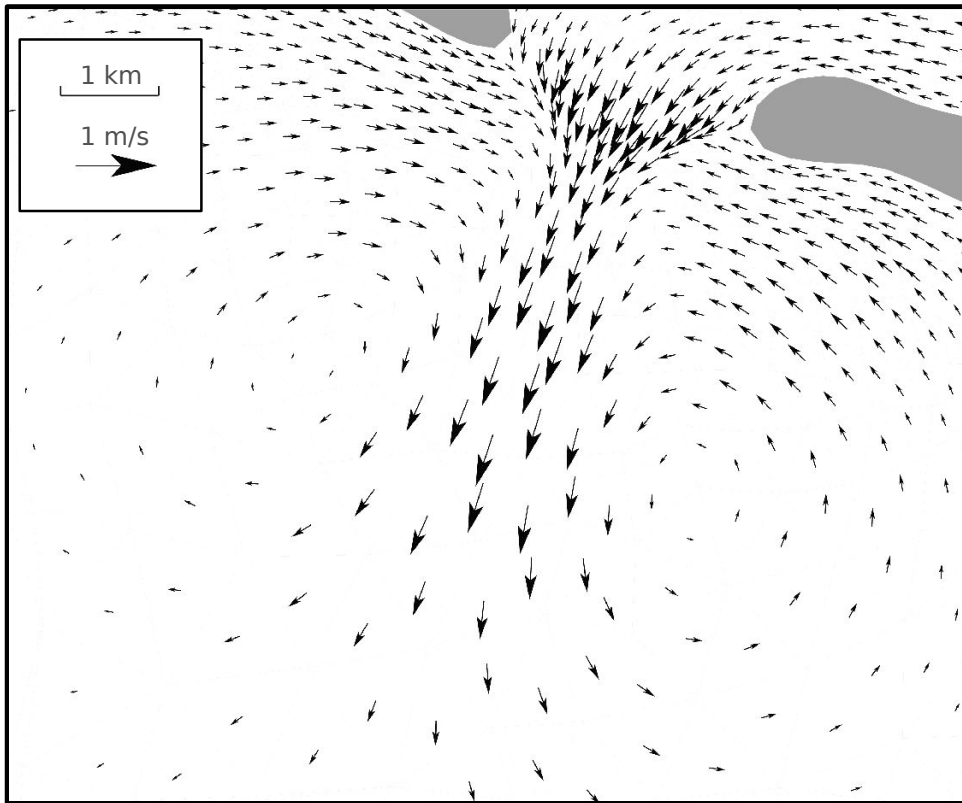


Figure 8. Tidal jets and eddies due to the interaction of the flow with the topography near the open-sea boundary ( $14^{\circ}17'S$   $145^{\circ}08'E$ ).

drag from reefs is then much larger than the drag from muddy or sandy sea beds, according to Lugo Fernandez et al. (1998) and Roberts et al. (1975). Therefore, incorporating variable bottom friction coefficient and adapting the subgrid viscosity model could render the model more realistic as a predictive tool for ecohydrological applications.

### Acknowledgements

Eric Deleersnijder is a Research Associate with the Belgian National Fund for Scientific Research (FNRS). The present study was carried out within the scope of the project “A second-generation model of the ocean system”, which is funded by the *Communauté Française de Belgique*, as *Actions de Recherche Concertées*, under contract ARC 04/09-316. This work is a contribution to the development of SLIM, the Second-generation Louvain-la-Neuve Ice-ocean Model. Emmanuel Hanert thanks the Nuffield Foundation for a newly appointed lecturer award.

## References

- Armsworth, P., Bode, L., 1999. The consequences of non-passive advection and directed motion for population dynamics. *Proceedings of the Royal Society of London Seris A-Mathematica, Physical and Engineering Sciences* 455, 4045–4060.
- Bell, R., Elmetri, I., 1995. Ecological indicators of large-scale eutrophication in the great barrier reef lagoon. *Ambio* 24, 208215.
- Bernard, P.-E., Chevaugéon, N., Legat, V., Deleersnijder, E., Remacle, J.-F., 2007. High-order  $h$ -adaptive discontinuous Galerkin methods for ocean modeling. *Ocean Dynamics* 57, 109–121.
- Birkeland, C.E., 1997. *Life and Death of Coral Reefs*. Chapman and Hall, New-York.
- Blayo, E., Debreu, L., 2005. Revisiting open boundary conditions from the point of view of characteristic variables. *Ocean Modelling* 9, 231–252.
- Brinkman, R., Wolanski, E., Deleersnijder, E., McAllister, F., Skirving, W., 2001. Oceanic inflow from the Coral Sea into the Great Barrier Reef. *Estuarine, Coastal and Shelf Science* 54, 655–668.
- Deleersnijder, E., Beckers, J.-M., 1992. On the use of the  $\sigma$ -coordinate system in regions of large bathymetric variations. *Journal of Marine Systems* 3, 381–390.
- Done, T., 1988. Simulations of the recovery of pre-disturbance size structure in populations of porites spp. damaged by crown-of-thorns starfish. *Marine Biology* 100, 5161.
- Falconer, R. A., Wolanski, E., Mardapitta-Hadjipandeli, 1986. Modeling tidal circulation in an island's wake. *Journal of Waterway, Port, Coastal and Ocean Engineering* 112,2.
- Flather, R.A., 1976. A tidal model of the north-west european continental shelf. *Mémoires de la Société Royale des Sciences Liège* 6(10), 141–164.
- Fox, A.D., Maskell, S.K., 1995. Two-way interactive nesting of primitive equation ocean models with topography. *Journal of Physical Oceanography* 25, 2977–2996.
- Hamner, W., Hauri, I., 1981. Effect of island mass: water flow and plankton pattern around a reef in the great barrier reef lagoon. *Limnology & Oceanography* 26, 10841102.
- Hanert, E., Le Roux, D.Y., Legat, V., Deleersnijder, E., 2004. Advection schemes for unstructured grid ocean modelling. *Ocean Modelling* 7, 39–58, doi:10.1016/S1463-5003(03)00029-5.
- Hanert, E., Le Roux, D.Y., Legat, V., Deleersnijder, E., 2005. An efficient Eulerian finite element method for the shallow water equations. *Ocean Modelling* 10, 115–136, doi:10.1016/j.ocemod.2004.06.006.
- Hua, B.L., Thomasset, F., 1984. A noise-free finite element scheme for the two-layer shallow water equations. *Tellus* 36A, 157–165.
- Kalnay, E., Kanamitsu, M., Kistler, R., Collins, W., Deaven, D., Gandin, L., Iredell, M., Saha, S., White, G., Woollen, J., Zhu, Y., Leetmaa, A., Reynolds, B., Cheliah, M., Ebisuzaki, W., Higgins, W., Janowiak, J., Mo, K.C., Ropelewski, C.,

- Wang, J., Jenne, R., Joseph, D., 1996. The ncep/ncar 40-year reanalysis project. *Bull. Amer. Meteor. Soc.* 77, 437–470.
- King, B., 1992. A predictive model of the currents in Cleveland bay. American Society of Civil Engineers, *Estuarine and Coastal Modeling*, New-York.
- King, B. A., Wolanski, E., 1996. Tidal current variability in the central great barrier reef. *Journal of Marine Systems* 9, 187–202.
- Le Roux, D.Y., 2005. Dispersion relation analysis of the  $P_1^{nc} - P_1$  finite-element pair in shallow-water models. *SIAM Journal of Scientific Computing* 27, 394–414, doi: 10.1137/030602435.
- Legrand, S., Deleersnijder, E., Hanert, E., Legat, V., Wolanski, E., 2006. High-resolution, unstructured meshes for hydrodynamic models of the Great Barrier Reef, Australia. *Estuarine, Coastal and Shelf Science* 68, 36–46.
- Lugo Fernandez, A., Roberts, H.H., Wiseman, W.J., Carter, B.L., 1998. Water level and currents of tidal and infragravity periods at Tague Reef, St. Croix (USVI). *Coral Reefs* 17, 343–349.
- Luick, J. L., Mason, L., Hardy, T., Furnas, M. J., 2007. Circulation in the great barrier reef lagoon using numerical tracers and in situ data. *Continental Shelf Research* 27, 757–778.
- Monismith, S.G., 2007. Hydrodynamics of coral reefs. *Annual Review of Fluid Mechanics* 39, 37–55.
- Okubo, A., 1971. Oceanic diffusion diagrams. *Deep Sea Research* 18, 789–802.
- Pattiaratchi, C., James, A., Collins, M., 1986. Island wakes and headland eddies: a comparison between remotely sensed data and laboratory experiments. *Journal of Geophysical Research* 92, 783–794.
- Pietrzak, J., Deleersnijder, E., Schroeter, J. E., 2005. The second international workshop on unstructured mesh numerical modelling of coastal, shelf and ocean flows. *Ocean Modelling (special issue)* 10, 1–252.
- Reid, R.O., Bodine, B.R., 1968. Numerical model for storms sturges in galveston bay. American Society of Civil Engineers, *Journal Waterways Harbors Div.* 94, 33–57.
- Remacle, J.-F., 2007. Gmsh: a three-dimensional finite element mesh generator with built-in pre- and post-processing facilities. In preparation. <http://www.geuz.org/gmsh>.
- Richmond, R., Teina, R., Golbuu, Y., Victor, S., Idechong, N., Davis, G., Kotska, W., Neth, L., H., H., Wolanski, E., 2007. Watersheds and coral reefs: Conservation science, policy and implication. *Bioscience*, in press.
- Richmond, R.H., 1993. Coral reefs: present problems and future concerns resulting from anthropogenic disturbance. *Am. Zool.* 33, 54–57.
- Roberts, H.H., Murray, S.P., Suhayda, J.H., 1975. Physical process in a fringing reef system. *Journal of Marine Research* 33, 233–260.
- Smith, S.D., Banke, E.G., 1975. Variation of the sea surface drag coefficient with wind speed. *Quart. J. Roy. Met. Soc.* 101.
- Spagnol, S., Wolanski, E., E., D., 2001. Steering by coral reef assemblages. Wolanski, E. (Ed.) (2001). *Oceanographic processes of coral reefs: physical and biological links in the Great Barrier Reef*, CRC Press, Boca Raton, Florida, 231–236.

- Spall, M.A., Holland, W.R., 1991. A nested primitive equation model for oceanic applications. *Journal of Physical Oceanography* 21, 205–220.
- Veron, J.E.N., 1995. *Corals in Space and Time*. University of New South Wales Press, Sidney.
- Walters, R., 2005. Coastal ocean models: Two useful finite element methods. *Continental Shelf Research* 25, 775793.
- White, L., Deleersnijder, E., 2006. Diagnoses of vertical transport in a three-dimensional finite element model of the tidal circulation around an island. *Estuarine, Coastal and Shelf Science*, in press.
- White, L., Wolanski, E., 2007. Flow separation and vertical motions in a tidal flow interacting with a shallow-water island. *Estuarine, Coastal and Shelf Science*, (submitted).
- Wilkinson, C.R., 1999. Global and local threats to coral reef functioning and existence: review and predictions. *Marine Freshwater Resources* 50, 867–878.
- Wolanski, E., 1994. *Physical Oceanographic Processes of the Great Barrier Reef*. Boca Raton, FL: CRC Press.
- Wolanski, E., 2001. *Oceanographic Processes of Coral Reefs. Physical and Biological Links in the Great Barrier Reef*. CRC Press, Boca Raton.
- Wolanski, E., Asaeda, T., Tanaka, T., Deleersnijder, E., 1996. Three-dimensional island wakes in the field, laboratory and numerical codes. *Continental Shelf Research* 16, 1437–1452.
- Wolanski, E., Brinkmann, R., Spagnol, S., McAllister, F., Skirving, C. S. W., Deleersnijder, E., 2003a. Merging scales in models of water circulation: Perspectives from the Great Barrier Reef. In: Lakhan, V. (Ed.), *Advances in Coastal Modeling*. Elsevier, pp. 411–429.
- Wolanski, E., De'ath, G., 2005. Predicting the impact of present and future human land-use on the great barrier reef. *Estuarine, Coastal and Shelf Science* 64, 504–508.
- Wolanski, E., Doherty, P., Carleton, J., 1997. Directional swimming of fish larvae determines connectivity of fish populations on the great barrier reef. *Naturwissenschaften* 84, 262268.
- Wolanski, E., Drew, E., Abel, K., O'Brien, J., 1988. Tidal jets, nutrient upwelling and their influence on the productivity of the algal halimeda in the ribbon reefs, great barrier reef. *Estuarine, Coastal and Shelf Science* 26, 169–201.
- Wolanski, E., Hamner, W.M., 1988. Topographically controlled fronts in the ocean and their biological influence. *Science* 241, 177–181.
- Wolanski, E., Imberger, J., Heron, M. L., 1984. Island wakes in shallow coastal waters. *Journal of Geophysical Research* 20, 10,553–10,569.
- Wolanski, E., King, B., Spagnol, S., 1999. *Perspectives in Integrated Coastal Zone Management*. Springer-Verlag, Berlin.
- Wolanski, E., Marshall, K., Spagnol, S., 2003b. Nepheloid layer dynamics in coastal waters of the great barrier reef, australia. *Journal of Coastal Research* 19, 748752.
- Wolanski, E., Richmond, R., Davis, G., Deleersnijder, E., Leben, R., 2003c. Eddies around guam, an island in the mariana islands group. *Continental Shelf Research*

23, 991–1003.

Wolanski, E., Spagnol, S., 2000. Sticky waters in the Great Barrier Reef. *Estuarine, Coastal and Shelf Science* 50, 27–32.

Wolanski, E., Williams, D., Spagnol, S., Chanson, H., 2004. Undular tidal bore dynamics in the daly estuary, northern australia. *Estuarine, Coastal and Shelf Science* 60, 629–636.